Received: 4 May 2022 | Revised: 20 June 2022 | Accepted: 3 July 2022

DOI: 10.1111/acel.13676

Aging Cell WILEY

RESEARCH ARTICLE

Senolytic treatment reduces cell senescence and necroptosis in Sod1 knockout mice that is associated with reduced inflammation and hepatocellular carcinoma

Nidheesh Thadathil[1] | Ramasamy Selvarani[1] | Sabira Mohammed[1,2] | Evan H. Nicklas[1] | Albert L. Tran[1] | Maria Kamal[3] | Wenyi Luo[3] | Jacob L. Brown[4,5] | Marcus M. Lawrence[4,6] | Agnieszka K. Borowik[4] | Benjamin F. Miller[4,5,7] | Holly Van Remmen[4,5,7] | Arlan Richardson[1,2,5,7] | Sathyaseelan S. Deepa[1,2,7]

[1]Department of Biochemistry & Molecular Biology, University of Oklahoma Health Sciences Center, Oklahoma City, Oklahoma, USA

[2]Stephenson Cancer Center, University of Oklahoma Health Sciences Center, Oklahoma City, Oklahoma, USA

[3]Department of Pathology, University of Oklahoma Health Sciences Center, Oklahoma City, Oklahoma, USA

[4]Aging & Metabolism Program, Oklahoma Medical Research Foundation, Oklahoma City, Oklahoma, USA

[5]Oklahoma City VA Medical Center, Oklahoma City, Oklahoma, USA

[6]Department of Kinesiology and Outdoor Recreation, Southern Utah University, Cedar City, Utah, USA

[7]Center for Geroscience and Healthy Brain Aging, University of Oklahoma Health Sciences Center, Oklahoma City, Oklahoma, USA

Correspondence
Arlan Richardson, Department of Biochemistry and Molecular Biology, University of Oklahoma Health Sciences Center, 975 NE 10th Street, BRC-1374A, Oklahoma City, OK 73104, USA.
Email: arlan-richardson@ouhsc.edu

Sathyaseelan S. Deepa, Department of Biochemistry and Molecular Biology, University of Oklahoma Health Sciences Center, 975 NE 10th Street, BRC-1368A, Oklahoma City, OK 73104, USA.
Email: deepa-sathyaseelan@ouhsc.edu

Funding information
National Institute on Aging, Grant/Award Number: T32AG052363; U.S. Department of Veterans Affairs, Grant/Award Number: 1IK6 BX005234, 1IK6BX005238, I01 BX004453 and I01BX004538; American Physiological Society; University of Oklahoma Health Sciences Center; Presbyterian Health Foundation Seed; GeroOncology Pilot Grant; NIH, Grant/Award Number: R01AG064951, R01AG057424 and R01AG059718

Abstract

The goal of this study was to test the role cellular senescence plays in the increased inflammation, chronic liver disease, and hepatocellular carcinoma seen in mice null for Cu/Zn-Superoxide dismutase (Sod1KO). To inhibit senescence, wildtype (WT) and Sod1KO mice were given the senolytics, dasatinib, and quercetin (D + Q) at 6 months of age when the Sod1KO mice begin exhibiting signs of accelerated aging. Seven months of D + Q treatment reduced the expression of p16 in the livers of Sod1KO mice to WT levels and the expression of several senescence-associated secretory phenotype factors (IL-6, IL-1β, CXCL-1, and GDF-15). D + Q treatment also reduced markers of inflammation in livers of the Sod1KO mice, for example, cytokines, chemokines, macrophage levels, and Kupffer cell clusters. D + Q treatment had no effect on various markers of liver fibrosis in the Sod1KO mice but reduced the expression of genes involved in liver cancer and dramatically reduced the incidence of hepatocellular carcinoma. Surprisingly, D + Q also reduced markers of necroptosis (phosphorylated and oligomerized MLKL) in the Sod1KO mice to WT levels. We also found that inhibiting necroptosis in the Sod1KO mice with necrostatin-1s reduced the markers of cellular senescence (p16, p21, and p53). Our study suggests that an interaction occurs

Abbreviations: AFP, α-fetoprotein; ALT, alanine aminotransferase; D + Q, dasatinib and quercetin; DAMPs, damage-associated molecular patterns; H & E, hematoxylin and eosin; Nec-1s, necrostatin-1; OMRF, Oklahoma Medical Research Foundation; SASP, senescence-associated secretory phenotype; Sod1KO, Cu/Zn-superoxide dismutase knockout; WT, wildtype.

between cellular senescence and necroptosis in the liver of Sod1KO mice. We propose that these two cell fates interact through a positive feedback loop resulting in a cycle amplifying both cellular senescence and necroptosis leading to inflammaging and age-associated pathology in the Sod1KO mice.

KEYWORDS
cell senescence, Cu/Zn superoxide dismutase, hepatocellular carcinoma, inflammation, necroptosis, senolytics

1 | INTRODUCTION

Cu/Zn-superoxide dismutase is the major superoxide dismutase isozyme catalyzing the conversion of superoxide anions to hydrogen peroxide. It is found in all cells and is localized in the cytosol and the intermembrane space of the mitochondria (Okado-Matsumoto & Fridovich, 2001). Reaume et al. (1996), generated mice null for Cu/Zn-superoxide dismutase (Sod1KO) and reported that the Sod1KO mice appear normal at birth. However, the Sod1KO mice have very high levels of oxidative stress as measured by oxidative damage in various tissues and plasma (Muller et al., 2006). In addition, the lifespan of the Sod1KO mice was ~25% shorter than wildtype (WT) mice, with the median lifespan reduced from ~30 months for WT mice to ~22 months for Sod1KO mice (Elchuri et al., 2005; Zhang et al., 2013). Early studies showed that the Sod1KO mice exhibited various accelerated aging phenotypes, such as hearing loss (Keithley et al., 2005), cataracts (Olofsson et al., 2007), skin thinning and delayed wound healing (Iuchi et al., 2010), and sarcopenia (Muller et al., 2006). Our group showed that the Sod1KO mice also exhibited an accelerated loss of physical performance compared to age-matched WT mice as measured by voluntary running wheel activity, rota-rod performance, endurance exercise capacity, and grip strength (Deepa et al., 2017). More recently, we found that the overall severity of pathological lesions of Sod1KO mice was dramatically increased in adult Sod1KO mice compared to WT mice as measured by the geropathology grading score (Snider et al., 2018), which specifically assesses age-related pathological lesions. The Sod1KO mice also show an accelerated decrease in cognition compared to WT mice (Logan et al., 2019). These data strongly suggest that the Sod1KO mice are a model of accelerated aging. The Sod1KO mice also develop chronic liver disease, such as fatty liver and liver fibrosis (Sakiyama et al., 2016; Uchiyama et al., 2006) and hepatocellular carcinoma, which is a major end-of-life pathology for the Sod1KO mice (Elchuri et al., 2005; Zhang et al., 2013).

We found that Sod1KO mice show a dramatic increase in circulating proinflammatory factors and increased markers of inflammation in various tissues (Mohammed, Nicklas, et al., 2021; Zhang et al., 2017). Because chronic, sterile inflammation (inflammaging) is believed to play an important role in aging and many age-related diseases, such as cancer, we proposed that increased inflammation in the Sod1KO mice was an important factor in the accelerated aging phenotype (Zhang et al., 2017). One of the pathways believed to play a role in inflammaging is cellular senescence (Olivieri et al., 2018; Wiley & Campisi, 2021). We found that markers of cellular senescence (p16, p21, and SA-βGal) were increased in kidney tissue from Sod1KO mice and reduced by dietary restriction (Zhang et al., 2017), which increased the lifespan of Sod1KO mice (Zhang et al., 2013). Importantly, the changes in p16 and p21 were associated with changes in the expression of proinflammatory cytokines (e.g., IL-6, and IL-1β) in kidney and circulating cytokines (Zhang et al., 2017). Based on these data, we proposed that cellular senescence may be an important contributing factor to the accelerated aging phenotype observed in Sod1KO mice.

Recently, our attention turned to the potential role of necroptosis in inflammaging because it is a form of cell death that is highly proinflammatory due to the release of cell debris and self-molecules, damage-associated molecular patterns (DAMPs) (Pasparakis & Vandenabeele, 2015). We found that necroptosis was dramatically increased in the livers of Sod1KO mice, was associated with the increased inflammation and chronic liver disease, and treating Sod1KO mice with necrostatin-1s (Nec-1s), an inhibitor of necroptosis (Takahashi et al., 2012), reduced necroptosis and markers of inflammation in the liver (Mohammed, Nicklas, et al., 2021).

To gain a better understanding of the role cellular senescence plays in increased inflammation in Sod1KO mice, we treated Sod1KO mice with senolytics (dasatinib and quercetin, D + Q) to eliminate senescence cells (Zhu et al., 2015). We found that D + Q reduced inflammation and hepatocellular carcinoma in livers of the Sod1KO mice; however, we also found that D + Q also reduced markers of necroptosis in the livers of Sod1KO mice.

2 | RESULTS

2.1 | D + Q treatment reduces markers of cellular senescence in livers of Sod1KO mice

Female Sod1KO and WT mice were given D + Q starting at 6 months of age to avoid effects on development and when the Sod1KO mice begin to exhibit symptoms of accelerated aging, for example, muscle mass loss, weakness, and innervation, increased oxidative damage, and changes in mitochondrial function (Deepa

et al., 2017; Muller et al., 2006). D+Q was administered for 7 months using the protocol developed by Kirkland's group, which was shown to eliminate senescence cells in vivo (Zhu et al., 2015) and extend the healthspan and lifespan of 20-month-old WT mice (Xu et al., 2018). In this study, we focused on liver because cellular senescence and inflammation are increased in the livers of Sod1KO mice (Mohammed, Nicklas, et al., 2021) and because the Sod1KO mice develop fibrosis and hepatocellular carcinoma, which could arise from the increased cellular senescence and inflammation. Figure 1a shows that p16 and p21 transcripts are increased significantly in the livers of the Sod1KO mice as we have previously reported in male Sod1KO mice (Mohammed, Nicklas, et al., 2021). D+Q treatment significantly reduced the level of p16 transcripts to that observed in the WT mice; however, the expression of p21 was not significantly reduced by D+Q treatment. We also measured the expression of 12 of the senescent-associated secretory phenotype (SASP) factors commonly expressed by senescent cells (Acosta et al., 2008; Coppé et al., 2008). D+Q significantly reduced the expression of IL-6, IL-1β, CXCL-1, and GDF-15 in the livers of Sod1KO mice (Figure 1b,c).

2.2 | D+Q treatment reduces markers of inflammation in the livers of Sod1KO mice

We next studied the effect of D+Q treatment on markers of inflammation in the liver because cellular senescence has been associated with increased inflammation (Olivieri et al., 2018; Wiley & Campisi, 2021) and because Sod1KO mice show an increase in various markers of inflammation in liver (Mohammed, Nicklas, et al., 2021) and kidney (Zhang et al., 2017). Figure 2a shows the heat map for 84 proinflammatory cytokines and chemokines expressed in the livers of WT and Sod1KO mice treated with vehicle or D+Q. The data generated from the mouse cytokines and chemokines array are included in Table S1 in the supplement. It is evident that liver tissue from Sod1KO mice showed a dramatic increase in a large number of cytokines and chemokines compared to WT mice and that D+Q reduced the expression of most of these cytokines and chemokines. Figure 2b shows the quantification of the expression of 10 of the chemokines that showed a statistically significant increase in expression in the livers of the Sod1KO mice. The expression of nine of the 10 chemokines was significantly reduced (from 9% to 70%) by

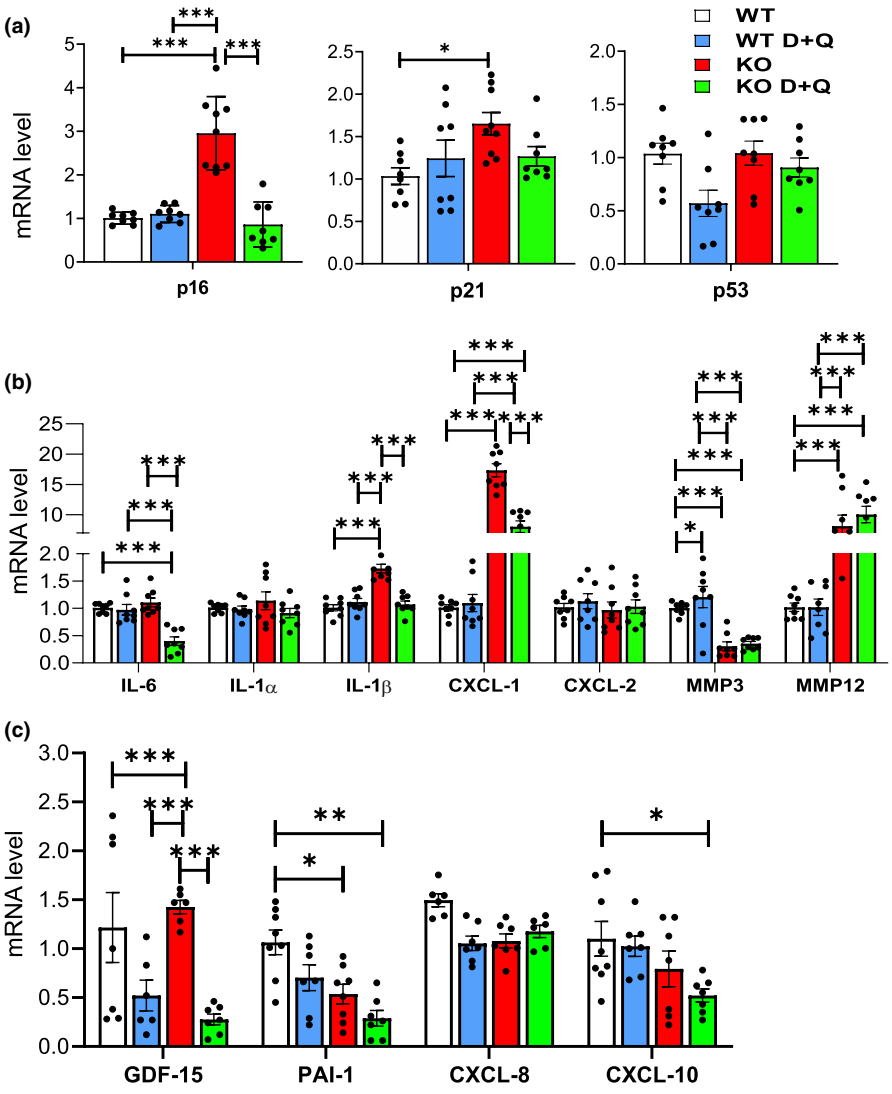

FIGURE 1 D+Q treatment significantly reduces markers of senescence and SASP factors in the livers of Sod1KO mice. Panel (a) shows transcript levels of $p16^{Ink4a}$ (*Cdkn2a*), $p21^{Cip1}$ (*Cdkn1a*), and p53. Panels (b, c) show the transcript levels of SASP factors. The data in the graphs are generated using liver tissue from WT mice treated with vehicle (white bars), WT mice treated with D+Q (blue bars), Sod1KO treated with vehicle (red bars), and Sod1KO mice treated with D+Q (green bars). Data were obtained from 6 to 8 mice per group and are expressed as the mean ± SEM. (ANOVA, ***$p \leq 0.0005$, **$p \leq 0.005$, *$p \leq 0.05$). D+Q, dasatinib and quercetin; SASP, senescence-associated secretory phenotype; Sod1KO, Cu/Zn-Superoxide dismutase

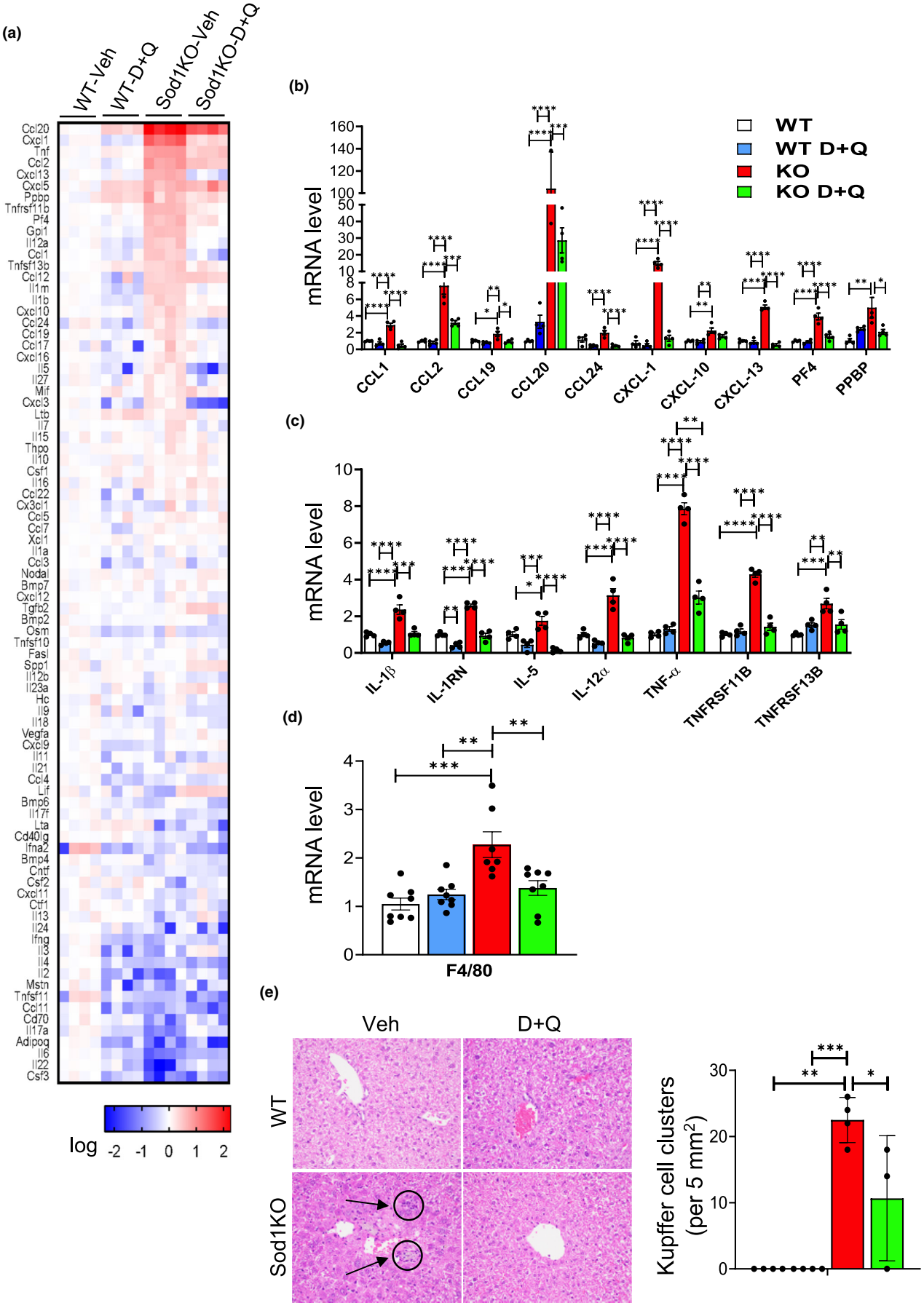
(a)
WT-Veh
WT-D+Q
Sod1KO-Veh
Sod1KO-D+Q
Ccl20
Cxcl1
Tnf
Ccl2
Cxcl13
Cxcl5
Ppbp
Tnfrsf11b
Pf4
Gpi1
Il12a
Ccl1
Tnfsf13b
Ccl12
Il1rn
Il1b
Cxcl10
Ccl24
Ccl19
Ccl17
Cxcl16
Il5
Il27
Mif
Cxcl3
Ltb
Il7
Il15
Thpo
Il10
Csf1
Il16
Ccl22
Cx3cl1
Ccl5
Ccl7
Xcl1
Il1a
Ccl3
Nodal
Bmp7
Cxcl12
Tgfb2
Bmp2
Osm
Tnfsf10
Fasl
Spp1
Il12b
Il23a
Hc
Il9
Il18
Vegfa
Cxcl9
Il11
Il21
Ccl4
Lif
Bmp6
Il17f
Lta
Cd40lg
Ifna2
Bmp4
Cntf
Csf2
Cxcl11
Ctf1
Il13
Il24
Ifng
Il3
Il4
Il2
Mstn
Tnfsf11
Ccl11
Cd70
Il17a
Adipoq
Il6
Il22
Csf3
log -2 -1 0 1 2
(b)
mRNA level
WT
WT D+Q
KO
KO D+Q
CCL1
CCL2
CCL19
CCL20
CCL24
CXCL-1
CXCL-10
CXCL-13
PF4
PPBP
(c)
mRNA level
IL-1β
IL-1RN
IL-5
IL-12α
TNF-α
TNFRSF11B
TNFRSF13B
(d)
mRNA level
F4/80
(e)
Veh
D+Q
WT
Sod1KO
Kupffer cell clusters (per 5 mm²)

FIGURE 2 D + Q treatment significantly reduces markers of inflammation in the livers of Sod1KO mice. Panel (a) shows the heat map for the transcript levels of 84 cytokines and chemokines measured by the RT^2 profiler™ PCR Array for liver tissue from WT and Sod1KO mice treated with vehicle or D + Q. Transcript levels greater than the mean are shaded in red and those lower than the mean are shaded in blue. Panel (b) shows the expression of the 10 chemokines, and Panel (c) shows the expression of the seven cytokines from the Profiler™ PCR Arrays that are significantly increased in the livers of the Sod1KO mice. The data were obtained from 4 to 6 mice per group and are expressed as mean ± SEM. Panel (d) shows the transcript levels of macrophage marker F4/80 in the livers of WT and Sod1KO mice treated with vehicle and/or D + Q. Data were obtained from 7 to 8 mice per group and are expressed as mean ± SEM. Panel (e) shows the detection of Kupffer cells cluster by H & E staining (left) and the quantification of Kupffer cell clusters in the livers WT and *Sod1*KO mice treated with vehicle or D + Q (right). Data were obtained from 3 to 5 mice per group and are expressed as the mean ± SEM. The data in the graphs are shown as follows: White bars for WT mice treated with vehicle, blue bars for WT mice treated with D + Q, red bars for Sod1KO treated with vehicle, and green bars for Sod1KO mice treated with D + Q. (ANOVA, ****$p < 0.0001$, ***$p \le 0.0005$, **$p \le 0.005$, *$p \le 0.05$). D + Q, dasatinib and quercetin; H & E, Hematoxylin and eosin; Sod1KO, Cu/Zn-Superoxide dismutase; WT, wildtype

FIGURE 3 D + Q treatment does not reduce fibrosis in the livers of Sod1KO mice. Panel (a) shows the serum levels of ALT expressed as IU/L. Panel (b) shows the lipid content in liver expressed as mg triglyceride/g of liver. Panel (c) shows the quantification of desmin by Western blots normalized to β-tubulin. Panel (d) shows transcript levels of *Col1α1* normalized to β-microglobulin and expressed as fold change. Panel (e) shows hydroxyproline levels expressed as μg of hydroxyproline/g of liver tissue. Panel (f) shows sections from picrosirius red staining (scale bar: 50 μm) (left) and the quantification of fibrotic area (right) for livers from WT and Sod1KO mice treated with vehicle or D + Q. The data in the graphs are shown as follows: White bars for WT mice treated with vehicle, blue bars for WT mice treated with D + Q, red bars for Sod1KO treated with vehicle, and green bars for Sod1KO mice treated with D + Q. The data were obtained from 6 to 12 mice per group and are expressed as the mean ± SEM. (ANOVA, ***$p \le 0.0005$, **$p \le 0.005$, *$p \le 0.05$). ALT, alanine aminotransferase; D + Q, dasatinib and quercetin; Sod1KO, Cu/Zn-Superoxide dismutase; WT, wildtype

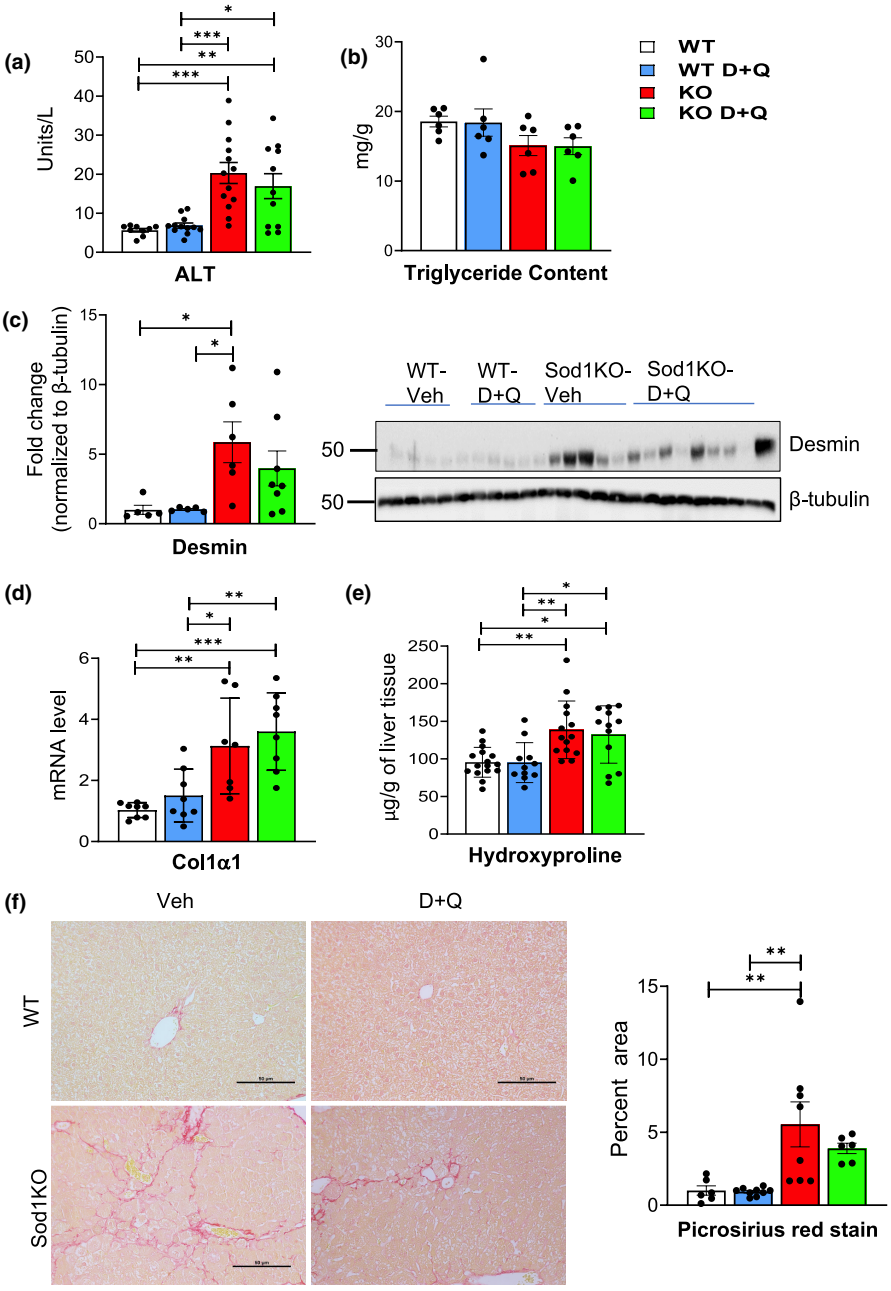

D + Q treatment. Figure 2c shows the quantification of the transcript levels of the seven cytokines that were significantly increased in the livers of the Sod1KO mice. D + Q treatment reduced the expression of all seven cytokines, and six of the cytokines were reduced to levels not significantly different from WT mice. Because macrophages are a major source of cytokines (Ju & Tacke, 2016) and because we

have shown that markers of macrophages are increased in the livers of Sod1KO mice (Mohammed, Nicklas, et al., 2021), we measured macrophage levels in the livers of WT and Sod1KO mice treated with vehicle or D+Q. Figure 2d shows the transcript levels of F4/80, a marker of macrophage levels. F4/80 transcript levels were increased in the Sod1KO mice and reduced by D+Q. The accumulation of clusters of Kupffer cells is also a measure of proinflammatory status of liver (Woltman et al., 2014). We histologically compared liver tissue from the four groups of mice for the presence of Kupffer cell clusters (Figure 2e). Few if any Kupffer cell clusters were observed in liver tissue from the WT mice; however, we observed Kupffer cell clusters in the livers of the Sod1KO mice that were reduced in the Sod1KO mice treated with D+Q.

2.3 | D+Q treatment has no impact on fibrosis in the livers of Sod1KO mice

We next determined if D+Q treatment had an impact on chronic liver disease, which is increased in the Sod1KO mice (Mohammed, Nicklas, et al., 2021; Sakiyama et al., 2016; Uchiyama et al., 2006). The data in Figure 3a show that circulating alanine aminotransferase (ALT) levels, which is a measure of liver damage, are increased in the Sod1KO mice as previously observed (Mohammed, Nicklas, et al., 2021). However, ALT levels were not significantly altered by D+Q treatment. We also measured the accumulation of lipid in the livers of the WT and Sod1KO mice as measured by triglyceride content (Figure 3b). We observed no significant differences in the triglyceride content of livers from WT and Sod1KO mice with and without D+Q treatment. Sakiyama et al. (2016) also observed no significant difference in the triglyceride content of livers from WT and Sod1KO mice when fed normal chow diet. We next measured various markers of fibrosis in the four groups of mice. The activation and proliferation of stellate cells play a major role in the pathogenesis of hepatic fibrosis (Guido et al., 1996), and activated stellate cells up-regulate the expression of desmin (Kim et al., 2012). Figure 3c shows that desmin levels are increased over five-fold in liver tissue from Sod1KO mice compared to WT mice; however, D+Q treatment did not significantly reduce desmin levels in the Sod1KO mice. We also measured other markers of fibrosis in liver tissue from the four groups of mice: transcript levels of collagen 1α1 (*Col1α1*), hydroxyproline levels, and histopathological changes. *Col1α1* expression (Figure 3c) and hydroxyproline levels (Figure 3d) were significantly increased in the livers of the Sod1KO mice, and D+Q treatment did not reduce these two markers of liver fibrosis. Histopathological evidence of liver fibrosis was assessed by the appearance of perisinusoidal/pericellular (chicken wire) fibrosis using Picrosirius Red staining (Figure 3e). This marker of fibrosis was increased in the livers of Sod1KO mice, and D+Q treatment had no significant effect on this pathological lesion. Thus, our data show that D+Q treatment had no impact on the increase in fibrosis observed in the Sod1KO mice.

2.4 | D+Q treatment reduces hepatocellular carcinoma in the livers of Sod1KO mice

Because hepatocellular carcinoma is a major pathology observed in Sod1KO mice (Elchuri et al., 2005; Zhang et al., 2013), we studied the impact of D+Q on the development of cancer in the livers of the Sod1KO mice. The increase in liver weight, which is characteristic of the Sod1KO mice and associated with the development of liver tumors, was reduced by D+Q treatment (Figure 4a) as was the increase in circulating levels of α-fetoprotein (AFP), a liver tumor marker (Figure 4b). Figure 4c shows the heat map for 84 genes involved in the progression of hepatocellular carcinoma and other forms of hepatocarcinogenesis. The data generated from the liver cancer array are included in Table S2 in the supplement. These genes are involved in signal transduction pathways commonly altered in cancer and genes involved in other dysregulated biological pathways such as epithelial to mesenchymal transition, cell cycle, apoptosis, and inflammation. In addition to liver tissue from the WT mice and non-tumor tissue from Sod1KO mice, we also studied tumor tissue from the Sod1KO mice. The expression of 20 genes was significantly up-regulated in tumor tissue from Sod1KO mice, and the expression of many of these genes was increased in non-tumor tissue from the Sod1KO mice. Figure 4d shows the expression of four genes that have been shown to play

FIGURE 4 Liver cancer is reduced in Sod1KO mice treated with D+Q. Panel (a) shows the liver weight normalized to body weight. Panel (b) shows AFP levels in the serum expressed as ng/ml. Panel (c) shows the heat map for the RT^2 Profiler™ PCR Arrays of 84 genes related to liver cancer for normal liver tissue from WT and Sod1KO mice treated with vehicle or D+Q as well as tumor tissue from Sod1KO mice treated with vehicle. Transcript levels greater than the mean are shaded in red and those lower than the mean are shaded in blue. Panel (d) shows the quantification of the fold change in mRNA levels for four genes (*Myc*, *Tgfbr2*, *Socs3*, and *Cdkn2a*) that were significantly increased in normal tissue from Sod1KO mice treated with vehicle. The data were obtained from 4 to 6 mice per group and are expressed as mean ± SEM. The data in the graphs in Panels (a, b, d) are shown as follows: Non-tumor tissue from WT mice treated with vehicle (white bars), WT mice treated with D+Q (blue bars), non-tumor tissue from Sod1KO treated with vehicle (red bars) or Sod1KO mice treated with D+Q (green bars), and tumor tissue from Sod1KO mice treated with vehicle (red bars with stripes). (ANOVA, $^{****}p < 0.0001$, $^{***}p \leq 0.0005$, $^{**}p \leq 0.005$, $^{*}p \leq 0.05$). Panel (e) graphically shows the number of WT and Sod1KO mice treated with vehicle or D+Q that showed the presence (red) or absence of hepatocellular carcinoma tumors (green). None of the WT mice treated with vehicle ($n = 15$) or D+Q ($n = 11$) showed the presence of tumors while seven of Sod1KO mice treated with vehicle ($n = 11$) and one of the Sod1KO mice treated with D+Q ($n = 13$) showed the presence of tumors. This decrease in tumors was significant at the $p < 0.0001$ level as determined by the chi-squared test. AFP, α-fetoprotein; D+Q, dasatinib and quercetin; Sod1KO, Cu/Zn-Superoxide dismutase; WT, wildtype

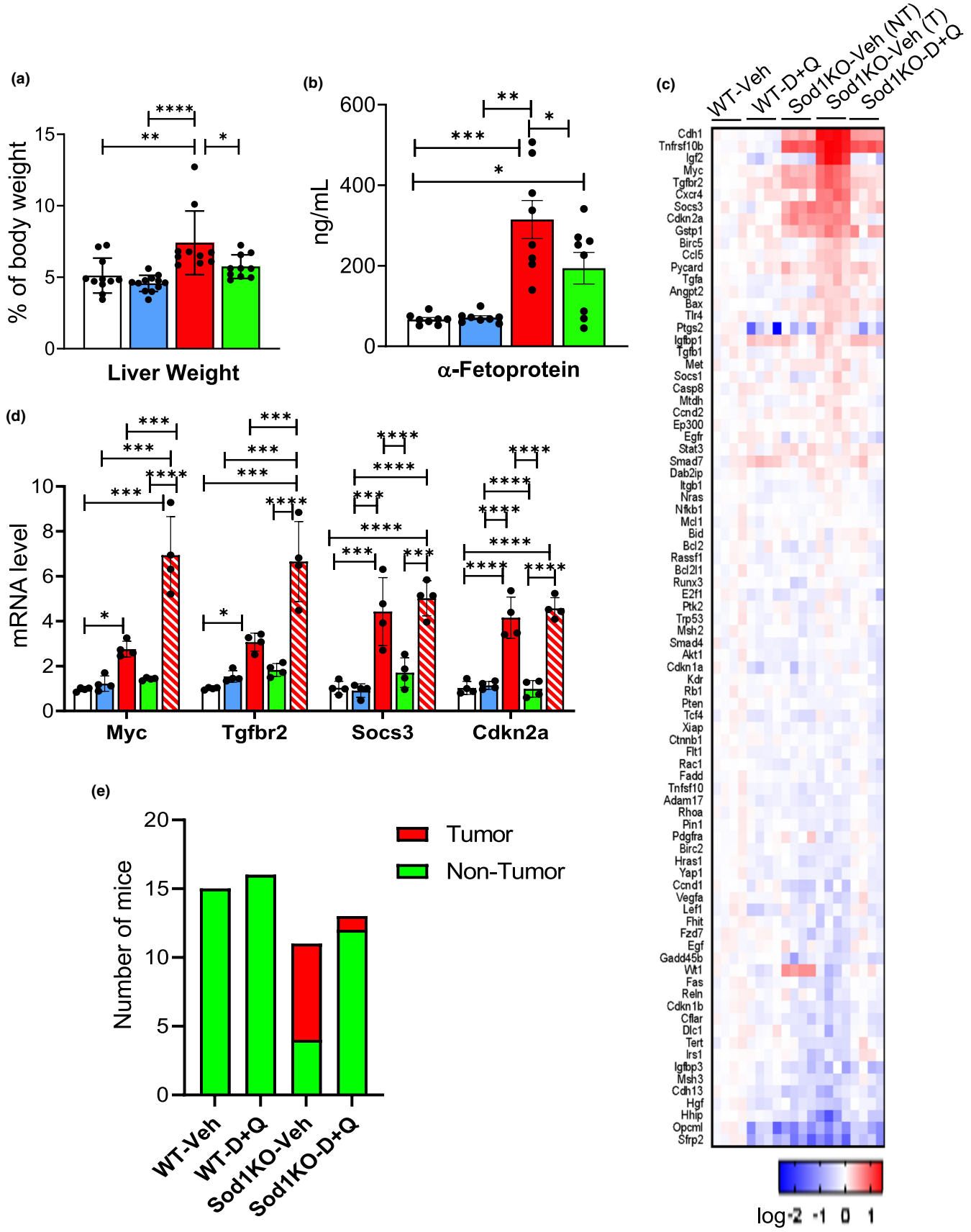

a role in liver cancer that were significantly increased in non-tumor and tumor tissue from Sod1KO mice: *Myc*, *Tgfbr2*, *Socs3*, and D + Q reduced the expression of these genes to the basal levels observed in the WT mice. We carefully checked the liver tissue from each of the mice used in the study for the presence of tumors, and as shown in Figure S1 in the supplement, these tumors expressed

markers specific for hepatocellular carcinoma, for example, glypican 3 and AFP (Zhao et al., 2013). Figure 4e shows the incidence of tumors in the WT and Sod1KO mice. As expected, we observed no tumors in any of the WT mice. However, 64% (7 out of 11) of the Sod1KO mice showed the presence of liver tumors. D + Q dramatically reduced the incidence of liver tumors in the Sod1KO mice to only 1 out of the 13 Sod1KO mice treated with D + Q.

2.5 | D + Q treatment reduces markers of necroptosis in the livers of Sod1KO mice

We also studied the impact of D + Q treatment on other cell fates because D + Q has been shown to alter apoptosis (Kirkland & Tchkonia, 2020) and because we have shown that necroptosis is increased in liver tissue from Sod1KO mice (Mohammed, Nicklas, et al., 2021). As shown in Figure 5a, we observed no significant change in cleaved caspase 3 activity, a marker of apoptosis, in the livers from the WT or Sod1KO mice. Next, we measured the level of necroptosis in liver tissue from the WT and Sod1KO mice by measuring the phosphorylation and oligomerization of MLKL, which is the terminal step in necroptosis resulting in the disruption of the cell membrane and release of DAMPs (Chen et al., 2014; Huang et al., 2017). A dramatic increase in P-MLKL levels (Figure 5b) and MLKL oligomerization (Figure 5c) was observed in the livers of the Sod1KO mice, which is consistent with our previously published data (Mohammed, Nicklas, et al., 2021). To our surprise, we observed that D + Q treatment reduced these markers of necroptosis in the Sod1KO mice to the levels observed in WT mice. Interestingly, the decrease in necroptosis in the D + Q treated Sod1KO mice was not associated with a decrease in liver damage as measured by serum ALT levels (Figure 3b).

Our data suggest that either D + Q inhibits necroptosis as well as cell senescence or that inhibiting cell senescence leads to reduced necroptosis, that is, there is an interaction between cell senescence and necroptosis where inhibiting one cell-fate impacts the other. To test the second possibility, we studied whether inhibiting necroptosis in the Sod1KO mice had an effect on cellular senescence. In these experiments, we used liver tissue from male Sod1KO mice used in a previous study, in which we showed that 25 days of Nec-1s treatment reduced necroptosis (Mohammed, Nicklas, et al., 2021). Figure 5d shows the expression of p16, p21, and p53 in liver tissue from these Sod1KO mice. Nec-1s treatment reduced p16, p21, and p53 transcript levels, demonstrating that inhibiting necroptosis in Sod1KO mice is also associated with reduced senescence.

3 | DISCUSSION

Chronic, low-grade inflammation that occurs with age (inflammaging) has been identified as one of the "seven pillars of aging" (Kennedy et al., 2014). Inflammaging has been observed in all mammalian species studied including rodents (Brubaker et al., 2011), rhesus monkeys (Didier et al., 2012), and humans (Franceschi & Campisi, 2014). Because inflammation is strongly associated with a variety of diseases, such as cardiovascular disease, cancer, type 2 diabetes, frailty, and neurodegenerative diseases, it has been argued that inflammaging is an important factor in the etiology of these diseases (Ferrucci & Fabbri, 2018; Franceschi & Campisi, 2014). In addition, studies with mice show that interventions that increase lifespan, such as dietary restriction (Spaulding et al., 1997), dwarfism (Masternak & Bartke, 2012), and rapamycin treatment (Richardson et al., 2015), reduce inflammation. On the contrary, Sod1KO mice, which show accelerated aging, exhibit an increase in markers of inflammation (Zhang et al., 2016). At the present time, several pathways have been proposed to play a role in inflammaging, and cellular senescence is one of these pathways (Olivieri et al., 2018; Wiley & Campisi, 2021). Cytokines and chemokines produced and secreted by senescent cells as part of the SASP have the potential to activate the immune system resulting in the generation of an inflammatory response. We previously found that markers of cellular senescence were higher in the Sod1KO mice and were reduced by dietary restriction, which was associated with an increase or decrease, respectively, in markers of inflammation (Zhang et al., 2016). These data led us to propose that cellular senescence played a role in increased inflammation and the accelerated aging phenotype observed in the Sod1KO mice.

The goal of this study was to test whether cellular senescence plays a role in the increase in inflammation and the progression of fibrosis and hepatocellular carcinoma observed in Sod1KO mice by treating Sod1KO mice with senolytics to eliminate senescent cells. Using a combination of dasatinib (a tyrosine kinase inhibitor) and quercetin (a flavonoid), we found that 7 months of D + Q treatment reduced the expression of p16 in the livers of Sod1KO mice to WT levels as well as reducing the transcript levels of several SASP factors. Importantly, we observed that D + Q treatment reduced markers of inflammation in liver supporting our proposal that cellular senescence was at least partially responsible for the increased hepatic inflammation observed in the Sod1KO mice. Because inflammation has been shown to play a role in liver fibrosis (Duval et al., 2015), we studied the effect of D + Q on fibrosis, which is increased in the livers of the Sod1KO mice (Mohammed, Nicklas, et al., 2021; Sakiyama et al., 2016; Uchiyama et al., 2006). We were surprised to find that D + Q treatment had no effect on the various markers of fibrosis we assessed. One possible explanation for the lack of an effect of D + Q on fibrosis was because fibrosis was already developed at 6 months of age in the Sod1KO mice before D + Q treatment. Consistent with this possibility is the report by Sakiyama et al. (2016) showing that increased collagen deposition in the livers of Sod1KO mice occurs as early as 3 months of age. We measured fibrosis (Col1a1 expression) in the livers of 6-month-old WT and Sod1KO mice, and as shown in Figure S2, the level of fibrosis was similar in the Sod1KO mice at 6 and 13 months of age. Thus, a reduction in cellular senescence and inflammation after 6 months of age does not impact fibrosis.

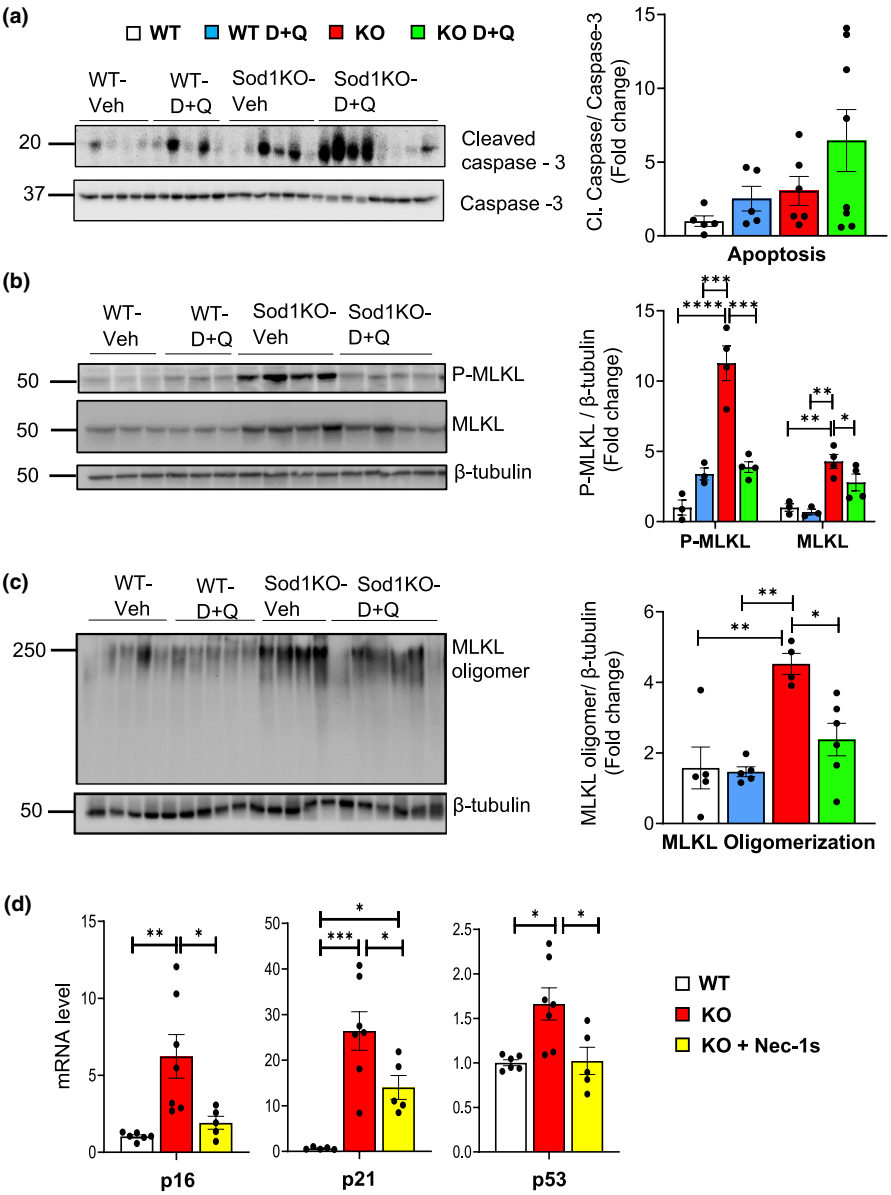

FIGURE 5 Impact of D + Q treatment on apoptosis and necroptosis and Nec-1s treatment on cellular senescence in the livers of Sod1KO mice. Panel (a) shows Western blots of cleaved caspase-3 and caspase-3 (left) and the quantification of cleaved caspase-3 normalized to caspase-3 (right). Panel (b) shows Western blots of P-MLKL, MLKL, and β-tubulin (left) and the quantification of P-MLKL and MLKL normalized to β-tubulin (right). Panel (c) shows Western blots of MLKL oligomers and β-tubulin (left) and the quantification of MLKL oligomers normalized to β-tubulin (right). The data in the graphs in Panels (a, b, d) are shown as follows: liver tissue from WT mice treated with vehicle (white bars), WT mice treated with D + Q (blue bars), Sod1KO treated with vehicle (red bars), and Sod1KO mice treated with D + Q (green bars). Panel (d) show the effect of Nec-1S treatment on markers of cellular senescence that was obtained from the livers of male WT and Sod1KO mice studied by Mohammed, Nicklas, et al. (2021). The data in the graphs are shown as follows. WT treated with vehicle (white bars), Sod1KO treated with vehicle (red bars), and Sod1KO mice treated with Nec-1s (yellow bars). The data in all the graphs were obtained from 4 to 6 mice per group and are expressed as the mean ± SEM. (ANOVA, $^{****}p < 0.0001$, $^{***}p \leq 0.0005$, $^{**}p \leq 0.005$, $^{*}p \leq 0.05$). D + Q, dasatinib and quercetin; Nec-1s, necrostatin-1; Sod1KO, Cu/Zn-Superoxide dismutase; WT, wildtype

In contrast to fibrosis, we found that D + Q treatment reduced the expression of several genes involved in liver cancer as well as dramatically reducing the incidence of hepatocellular carcinoma in the Sod1KO mice. Chronic inflammation has been shown to play an important role in hepatocellular carcinoma. For example, higher baseline serum levels of inflammatory markers (CRP, IL-6, C-peptide) are associated with an increased risk of developing hepatocellular carcinoma in the general population (Aleksandrova et al., 2014), and the use of anti-inflammatory drugs is linked to lower risk and better survival in patients with hepatocellular carcinoma (Pang et al., 2017; Sahasrabuddhe et al., 2012; Tao et al., 2018). In addition, the enhanced production of proinflammatory cytokines TNF-α and IL-6 are key mediators of obesity-mediated hepatocellular carcinoma (Park et al., 2010; Villanueva & Luedde, 2016; Yu et al., 2018). Therefore,

our data are consistent with the reduction in inflammation and cellular senescence being responsible for the reduction of hepatocellular carcinoma observed in the D + Q treated Sod1KO. However, it is also possible that the reduction in hepatocellular carcinoma is due to a direct effect of dasatinib on the growth of cancer cells. Dasatinib is second generation tyrosine kinase inhibitor that downregulates various tyrosine kinases containing BCR-ABL1 and kinases of SRC family, and it inhibits the growth of cancer cells (Zhang et al., 2020), including hepatocellular carcinoma cells (Chang & Wang, 2013; Liu et al., 2021).

Because we previously observed that both cellular senescence (Zhang et al., 2017) and necroptosis (Mohammed, Nicklas, et al., 2021) were increased in the Sod1KO mice, our goal in this study was to use D + Q treatment to differentiate the effect of cellular senescence and necroptosis on the increased inflammation observed in the Sod1KO mice. We were surprised to find that D + Q also reduced markers necroptosis in the Sod1KO mice. Thus, the decrease in inflammation observed in the D + Q treated Sod1KO mice could be due to cellular senescence, necroptosis, or both. While this result was surprising, it was not totally unexpected because we recently found that Nec-1s treatment, which inhibits necroptosis, reduced markers of both necroptosis and cell senescence in the livers of old mice (Mohammed, Thadathil, et al., 2021). We found in this study that Nec-1s treatment reduced markers of cellular senescence in the liver of Sod1KO mice. Thus, the data from our studies with D + Q and Nec-1s suggest that cellular senescence and necroptosis could be interacting through a positive feedback loop resulting in a cycle amplifying both cell fates leading to inflammaging and age-associated pathology. Senescent cells, which accumulate with age, could trigger necroptosis in surrounding cells by the paracrine/juxtracrine actions of the SASP factors (cytokines, chemokines, extracellular proteases, growth factors, lipids, etc.) secreted from senescent cells. For example, TNF-α, a component of SASP (Acosta et al., 2013; Freund et al., 2010), is a potent inducer of necroptosis (Liu et al., 2014; Vanlangenakker et al., 2011). Because senescent cells are resistant to apoptosis and accumulate with age, they are a potential source of factors that could push cells to undergo necroptosis in old animals or in Sod1KO mice leading to the release of DAMPs, which are potent inducers of inflammation (Kataoka et al., 2014; Zhang et al., 2010). The elimination of senescent cells in Sod1KO mice by D + Q treatment could therefore reduce necroptosis. In turn, DAMPs arising from necroptotic cells could increase the burden of senescent cells by inducing cells to undergo senescence. DAMPs, HMGB1, and IL-1 have been shown to induce cultured fibroblasts to undergo senescence (Acosta et al., 2013; Davalos et al., 2013). In addition, extracellular vesicles have been shown to induce cellular senescence (Borghesan et al., 2019), and extracellular vesicles are released during necroptosis (Yoon et al., 2017). Therefore, reducing necroptosis by Nec-1s could reduce the potential of DAMPs inducing cells to undergo senescence.

In summary, our study shows for the first time that the senolytics, D + Q not only reduce cellular senescence but also reduce necroptosis. We propose that the reduction in necroptosis by D + Q most likely arises from a reduction in the number of senescent cells that secrete SASP factors such as TNF-α, which induce cells to undergo necroptosis. Therefore, cell senescence and necroptosis could play an important role in inflammaging resulting in the progression of many age-related diseases and aging. Future experiments to define the potential interaction between cellular senescence and necroptosis should focus on determining the types of cells impacted by senescence and necroptosis and their interaction. For example, are same or different cell type(s) in the liver undergoing cell senescence and necroptosis, what is the tissue location of the senescent and necroptotic cells, do SASP factors induce necroptosis in cell cultures, and vice versa, do DAMPs released by necroptotic cells induce cellular senescence? In addition, it would be interesting to determine whether combining inhibitors of senescence and necroptosis are more effective in reducing the negative effects associated with senescence and necroptosis, for example, inflammaging.

4 | EXPERIMENTAL PROCEDURES

4.1 | Animals

The Sod1KO and WT mice were generated and raised in animal facilities at the Oklahoma Medical Research Foundation (OMRF), and all procedures were approved by the IACUC at OMRF. The mice were group housed in ventilated cages at 20 ± 2°C, on a 12-/12-h dark/light cycle, and fed a commercial rodent chow diet ad libitum. Four groups of female mice were used in the study: WT mice treated with vehicle, WT mice treated with D + Q, Sod1KO mice treated with vehicle, and Sod1KO mice treated with D + Q. At 6 months of age, mice were given dasatinib (5 mg/kg) and quercetin (50 mg/kg) dissolved in vehicle (10% ethanol, 30% polyethylene glycol 400 and 60% Phosal 50 PG) or vehicle by oral gavage as described by Zhu et al. (2015) for three constitutive days every 15 days over 7 months. The final dose of D + Q was given 7 days prior to sacrifice at 13 months of age. Liver tissue was collected, immediately frozen in liquid nitrogen, and stored at −80°C until use in the experiments described below.

4.2 | RNA isolation, cDNA synthesis, and quantitative real-time PCR

Real-time-PCR was performed using 20 mg frozen liver tissues as described previously by Mohammed, Nicklas, et al. (2021). Briefly, total RNA was extracted using RNeasy kit (Qiagen) as per manufacturer's instructions. First-strand cDNA was synthesized using a high-capacity cDNA reverse transcription kit (ThermoFisher Scientific), and quantitative RT-PCR was performed with Power SYBR Green PCR Master Mix (ThermoFischer Scientific). The primers used for RT-PCR analysis are given in Table S3 in the supplement. Calculations were performed by a comparative method ($2^{-\Delta\Delta}$Ct) using β-microglobulin or β-actin as controls as described previously (Mohammed, Nicklas, et al., 2021).

Genes involved in liver cancer were analyzed by Mouse RT^2 Profiler^{TCM} PCR Liver Cancer Array (Qiagen, Cat# PAMM-1332E-4 [330231]), which measures the expression of 84 genes involved in the progression of HCC, as well as other forms of hepatocarcinogenesis. Similarly, the RT^2 Profiler™ PCR Array Mouse Cytokines & Chemokines (Qiagen, Cat# PAMM-1502E-4 [330231]) was used to analyze the 84 cytokines and chemokines levels in the liver samples.

4.3 | Western blotting

Western blots were performed as described previously (Mohammed, Nicklas, et al., 2021; Mohammed, Thadathils, et al., 2021). Images were taken using ChemiDoc imaging system (Bio-Rad Laboratories) and quantified using ImageJ Software (U.S. National Institutes of Health). Primary antibodies against the following proteins were used: phospho(S345) MLKL from Abcam; MLKL from Millipore Sigma; Cleaved Caspase-3, and Caspase from 3 Cell Signaling Technology; desmin from ThermoFisher Scientific; β-tubulin from Sigma-Aldrich. HRP-linked anti-rabbit IgG, HRP-linked anti-mouse IgG, and HRP-linked anti-rat IgG from Cell Signaling Technology were used as secondary antibody.

4.4 | MLKL oligomerization

MLKL oligomerization was measured as described by Miyata et al. (2021). Briefly, liver tissue was homogenized in HEPES buffer (pH 7.4) and protein in the homogenate quantified using Bradford method. Protein samples were prepared using 2× Laemmli buffer without any reducing agents to maintain the proteins under non-reducing conditions. Forty μg of protein was resolved under non-reducing conditions without SDS in running buffer and polyacrylamide gel. MLKL oligomers were detected on the gels as larger than 200 kDa and quantified using the antibody to MLKL as described above.

4.5 | Histological examination of liver for clusters of Kupffer cells

Formalin-fixed liver tissue was embedded in paraffin, and 4 μm sections were generated using a microtome. Hematoxylin and eosin (H & E) staining was performed on the tissue samples using the standard procedure at the Stephenson Cancer Center Tissue Pathology Core. H & E-stained sections were digitally scanned at 10× and 20× magnifications using Nikon Ti Eclipse microscope (Nikon). Clusters of Kupffer cells in the liver tissue were identified by a pathologist, and the Kupffer cell clusters in tissue sections were measured in three random fields per sample and quantified using Image J software.

4.6 | Immunohistochemistry analysis for hepatocellular carcinoma

Immunohistochemistry staining was performed as described by Thadathil et al. (2021) with modifications. Briefly, 4 μm paraffin-embedded liver sections were deparaffinized using graded series of xylene and ethanol, and the antigen retrieval was performed with Proteinase K treatment. Liver sections were then permeabilized, blocked and incubated with primary antibodies against glypican-3 or AFP (Thermofisher Scientific). After washing, sections were incubated with HRP conjugated anti-mouse or anti-rabbit secondary antibodies for 1 h. The sections were then visualized using 3,3 diaminobenzidine followed by Mayer's Hematoxylin (Sigma-Aldrich) counterstaining. These sections were washed, dehydrated with gradient ethyl alcohol, cleared in xylene, and mounted using DPX mounting media. The images were taken using a Nikon Ti Eclipse microscope (Nikon) for 3 random fields per sample.

4.7 | Alanine aminotransferase (ALT) assay

The activity of ALT in the serum was measured using the assay kit from Cayman Chemical Company following manufacturer's instructions.

4.8 | Steatosis assay

The lipid content of the liver was measured by the triglyceride content (mg) using the Triglyceride Colorimetric Assay Kit (Item No. 10010303) assay according to the manufacturer's (Cayman Chemical) instructions.

4.9 | α-Fetoprotein assay

Serum AFP levels were quantified using the mouse AFP/AFP Quantikine ELISA Kit (R&D Systems) according to the manufacturer's instructions.

4.10 | Hydroxyproline assay

Hydroxyproline content was measured as described by Smith et al. (2016). Liver tissue (~250 mg) was pulverized using liquid nitrogen and was digested in 6-M hydrochloric acid overnight at 110°C. Ten ml of the digest was mixed with 150 μl of isopropanol, 75 μl of Solution A (1:4 mix of 7% Chloramine T [Sigma-Aldrich]), and acetate citrate buffer (containing 57 g sodium acetate anhydrous, 33.4 g citric acid monohydrate, 435 ml 1 M sodium hydroxide, and 385 ml isopropanol in 1 L of buffer). The mixture was

vigorously mixed and incubated at room temperature for 10 min. After incubation, 1 ml of Solution B (3:13 mix of Ehrlich's reagent [3 g p-dimethyl amino benzaldehyde, 10 ml absolute ethanol, 675 µl sulfuric acid] and isopropanol) was added, and the solution incubated at 58°C for 30 min. The reaction was stopped by placing on ice for 10 min. The absorbance at 558 nm was measured using 200 µl aliquot of the final reaction mixture in a Spectra Max M2 spectrophotometer (Molecular Devices). The absorbance values were converted into µg units using the 4-parameter standard curve generated using the standards and expressed as µg hydroxyproline/g of tissue.

4.11 | Picrosirius red staining

Formalin-fixed liver tissue was embedded in paraffin, and 4 µm sections were taken using a microtome. Picrosirius red staining was conducted using the standard protocol employed by the Imaging Core facility at the Oklahoma Medical Research Foundation. Briefly, formalin-fixed sections were deparaffinized and stained with Picrosirius Red for 1 h. Excess of Picrosirius Red was removed by rinsing in acidified water. Sections were dehydrated with ethanol and cleared with xylene. The images were taken using a Nikon Ti Eclipse microscope (Nikon) for three random fields per sample and quantified using Image J software.

4.12 | Statistical analyses

A one-way ANOVA with Tukey's post hoc test was used to analyze data. All data were analyzed, and graphs were compiled using GraphPad Prism.

AUTHOR CONTRIBUTIONS

Nidheesh Thadathil performed experiments, analyzed data, and prepared figures, Ramasamy Selvarani, Sabira Mohammed, and Albert L. Tran performed Western blots. Evan H. Nicklas performed the real-time qPCR. Maria Kamal and Wenyi Luo performed histopathological analysis and scoring of H&E staining sections, and Benjamin F. Miller performed the hydroxyproline assay. Holly Van Remmen was responsible for designing the D+Q study and Jacob L. Brown, Marcus M. Lawrence, and Agnieszka K. Borowik4 for treating the mice with vehicle and D+Q. Arlan Richardson and Sathyaseelan S. Deepa designed the experiments and wrote and edited the manuscript as a team.

ACKNOWLEDGMENTS

The authors would like to thank Stephenson Cancer Center Tissue Pathology Core for performing H & E staining and the Imaging Core facility at the Oklahoma Medical Research Foundation for performing Picrosirius red staining. The efforts of authors were supported by NIH grants R01AG059718 (S. S. D.), R01AG057424 (A. R.), and R01AG064951 (B. F. M.) as well as a GeroOncology Pilot Grant (S. S. D.), Presbyterian Health Foundation Seed grant (S. S. D.) from the University of Oklahoma Health Sciences Center. M. M. L. and J. L. B. were supported by NIA Training Grant T32AG052363, and M. M. L. was supported by an American Physiological Society Postdoctoral Fellowship. In addition, A. R. and H. V. R. were supported by the following grants from the Department of Veterans Affairs: Senior Career Research Awards 1IK6BX005238 (A. R.) and 1IK6 BX005234 (H. V. R.) and Merit grants I01BX004538 (A. R.) and I01 BX004453 (H. V. R.).

CONFLICT OF INTEREST

The authors declare no competing financial interests.

DATA AVAILABILITY STATEMENT

The data that support the findings of this study are available in the manuscript and supplementary material of this article. Correspondence and requests for information should be addressed to A. R. or S. S. D.

ORCID

Holly Van Remmen https://orcid.org/0000-0003-0883-0642
Arlan Richardson https://orcid.org/0000-0001-9622-7311
Sathyaseelan S. Deepa https://orcid.org/0000-0002-3669-4820

REFERENCES

Acosta, J. C., O'Loghlen, A., Banito, A., Guijarro, M. V., Augert, A., Raguz, S., Costa, M. D., Brown, C., Popov, N., Takatsu, Y., Melamed, J., Fagagna, F. A., Bernard, D., Hernando, E., & Gil, J. (2008). Chemokine signaling via the CXCR2 receptor reinforces senescence. *Cell*, *133*(6), 1006–1018. https://doi.org/10.1016/j.cell.2008.03.038

Acosta, J. C., Banito, A., Wuestefeld, T., Georgilis, A., Janich, P., Morton, J. P., Athineos, D., Kang, T. W., Lasitschka, F., Andrulis, M., Morris, K. J., Khan, S., Jin, H., Dharmalingam, G., Snijders, A. P., Carroll, T., Capper, D., Pritchard, C., … Gil, J. (2013). A complex secretory program orchestrated by the inflammasome controls paracrine senescence. *Nature Cell Biology*, *15*(8), 978–990. https://doi.org/10.1038/ncb2784

Aleksandrova, K., Boeing, H., Nöthlings, U., Jenab, M., Fedirko, V., Kaaks, R., Lukanova, A., Trichopoulou, A., Trichopoulos, D., Boffetta, P., Trepo, E., Westhpal, S., Duarte-Salles, T., Stepien, M., Overvad, K., Tjonneland, A., Halkjaer, J., Boutron-Ruault, M., Dossus, L., … Pischon, T. (2014). Inflammatory and metabolic biomarkers and risk of liver and biliary tract cancer. *Hepatology*, *60*(3), 858–871. https://doi.org/10.1002/hep.27016

Borghesan, M., Fafián-Labora, J., Eleftheriadou, O., Carpintero-Fernández, P., Paez-Ribes, M., Vizcay-Barrena, G., Swisa, A., Kolodkin-Gal, D., Ximenez-Embun, P., Lowe, R., Martin-Martin, B., Peinado, H., Munoz, J., Fleck, R. A., Dor, Y., Ben-Porath, I., Vossenkamper, A., Munoz-Espin, D., & O'Loghlen, A. (2019). Small extracellular vesicles are key regulators of non-cell autonomous intercellular communication in senescence via the interferon protein IFITM3. *Cell Reports*, *27*(13), 3956–3971.e6. https://doi.org/10.1016/j.celrep.2019.05.095

Brubaker, A. L., Palmer, J. L., & Kovacs, E. J. (2011). Age-related dysregulation of inflammation and innate immunity: Lessons learned from rodent models. *Aging and Disease*, *2*(5), 346–360.

Chang, A. Y., & Wang, M. (2013). Molecular mechanisms of action and potential biomarkers of growth inhibition of dasatinib (BMS-354825) on hepatocellular carcinoma cells. *BMC Cancer*, *13*, 267. https://doi.org/10.1186/1471-2407-13-267

Chen, X., Li, W., Ren, J., Huang, D., He, W.-T., Song, Y., Yang, C., Li, W., Zheng, X., Chen, P., & Han, J. (2014). Translocation of mixed lineage kinase domain-like protein to plasma membrane leads to necrotic cell death. *Cell Research*, *24*(1), 105–121. https://doi.org/10.1038/cr.2013.171

Coppé, J.-P., Patil, C. K., Rodier, F., Sun, Y., Muñoz, D. P., Goldstein, J., Nelson, P. S., & Campisi, J. (2008). Senescence-associated secretory phenotypes reveal cell-nonautonomous functions of oncogenic RAS and the p53 tumor suppressor. *PLoS Biology*, *6*(12), 2853–2868. https://doi.org/10.1371/journal.pbio.0060301

Davalos, A. R., Kawahara, M., Malhotra, G. K., Schaum, N., Huang, J., Ved, U., Beausejour, C. M., Coppe, J. P., Rodier, F., & Campisi, J. (2013). P53-dependent release of alarmin HMGB1 is a central mediator of senescent phenotypes. *The Journal of Cell Biology*, *201*(4), 613–629. https://doi.org/10.1083/jcb.201206006

Deepa, S. S., Bhaskaran, S., Espinoza, S., Brooks, S. V., McArdle, A., Jackson, M. J., Van Remmen, H., & Richardson, A. (2017). A new mouse model of frailty: The Cu/Zn superoxide dismutase knockout mouse. *GeroScience*, *39*(2), 187–198. https://doi.org/10.1007/s11357-017-9975-9

Didier, E. S., Sugimoto, C., Bowers, L. C., Khan, I. A., & Kuroda, M. J. (2012). Immune correlates of aging in outdoor-housed captive rhesus macaques (*Macaca mulatta*). *Immunity & Ageing*, *9*(1), 25. https://doi.org/10.1186/1742-4933-9-25

Duval, F., Moreno-Cuevas, J. E., González-Garza, M. T., Maldonado-Bernal, C., & Cruz-Vega, D. E. (2015). Liver fibrosis and mechanisms of the protective action of medicinal plants targeting inflammation and the immune response. *International Journal of Inflammation*, *2015*, 943497. https://doi.org/10.1155/2015/943497

Elchuri, S., Oberley, T. D., Qi, W., Eisenstein, R. S., Jackson Roberts, L., Van Remmen, H., Epstein, C. J., & Huang, T.-T. (2005). CuZnSOD deficiency leads to persistent and widespread oxidative damage and hepatocarcinogenesis later in life. *Oncogene*, *24*(3), 367–380. https://doi.org/10.1038/sj.onc.1208207

Ferrucci, L., & Fabbri, E. (2018). Inflammageing: Chronic inflammation in ageing, cardiovascular disease, and frailty. *Nature Reviews Cardiology*, *15*(9), 505–522. https://doi.org/10.1038/s41569-018-0064-2

Franceschi, C., & Campisi, J. (2014). Chronic inflammation (inflammaging) and its potential contribution to age-associated diseases. *The Journals of Gerontology Series A, Biological Sciences and Medical Sciences*, *69 Suppl 1*, S4–S9. https://doi.org/10.1093/gerona/glu057

Freund, A., Orjalo, A. V., Desprez, P.-Y., & Campisi, J. (2010). Inflammatory networks during cellular senescence: Causes and consequences. *Trends in Molecular Medicine*, *16*(5), 238–246. https://doi.org/10.1016/j.molmed.2010.03.003

Guido, M., Rugge, M., Chemello, L., Leandro, G., Fattovich, G., Giustina, G., Cassaro, M., & Alberti, A. (1996). Liver stellate cells in chronic viral hepatitis: The effect of interferon therapy. *Journal of Hepatology*, *24*(3), 301–307. https://doi.org/10.1016/s0168-8278(96)80008-0

Huang, D., Zheng, X., Wang, Z.-A., Chen, X., He, W.-T., Zhang, Y., Xu, J. G., Zhao, H., Shi, W., Wang, X., Zhu, Y., & Han, J. (2017). The MLKL channel in necroptosis is an octamer formed by tetramers in a dyadic process. *Molecular and Cellular Biology*, *37*(5), e00497-16. https://doi.org/10.1128/MCB.00497-16

Iuchi, Y., Roy, D., Okada, F., Kibe, N., Tsunoda, S., Suzuki, S., Takahashi, M., Yokoyama, H., Yoshitake, J., Kondo, S., & Fujii, J. (2010). Spontaneous skin damage and delayed wound healing in SOD1-deficient mice. *Molecular and Cellular Biochemistry*, *341*(1–2), 181–194. https://doi.org/10.1007/s11010-010-0449-y

Ju, C., & Tacke, F. (2016). Hepatic macrophages in homeostasis and liver diseases: From pathogenesis to novel therapeutic strategies. *Cellular & Molecular Immunology*, *13*(3), 316–327. https://doi.org/10.1038/cmi.2015.104

Kataoka, H., Kono, H., Patel, Z., Kimura, Y., & Rock, K. L. (2014). Evaluation of the contribution of multiple DAMPs and DAMP receptors in cell death-induced sterile inflammatory responses. *PLoS One*, *9*(8), e104741. https://doi.org/10.1371/journal.pone.0104741

Keithley, E. M., Canto, C., Zheng, Q. Y., Wang, X., Fischel-Ghodsian, N., & Johnson, K. R. (2005). Cu/Zn superoxide dismutase and age-related hearing loss. *Hearing Research*, *209*(1–2), 76–85. https://doi.org/10.1016/j.heares.2005.06.009

Kennedy, B. K., Berger, S. L., Brunet, A., Campisi, J., Cuervo, A. M., Epel, E. S., Franceschi, C., Lithgow, G. J., Morimoto, R. I., Pessin, J. E., Rando, T. A., Richardson, A., Schadt, E. E., Wyss-Coray, T., & Sierra, F. (2014). Geroscience: Linking aging to chronic disease. *Cell*, *159*(4), 709–713. https://doi.org/10.1016/j.cell.2014.10.039

Kim, S.-J., Ise, H., Goto, M., & Akaike, T. (2012). Interactions of vimentin- or desmin-expressing liver cells with N-acetylglucosamine-bearing polymers. *Biomaterials*, *33*(7), 2154–2164. https://doi.org/10.1016/j.biomaterials.2011.11.084

Kirkland, J. L., & Tchkonia, T. (2020). Senolytic drugs: From discovery to translation. *Journal of Internal Medicine*, *288*(5), 518–536. https://doi.org/10.1111/joim.13141

Liu, C., Zhu, X., Jia, Y., Chi, F., Qin, K., Pei, J., Zhang, C., Mu, X., Zhang, H., Dong, X., Xu, J., & Yu, B. (2021). Dasatinib inhibits proliferation of liver cancer cells, but activation of Akt/mTOR compromises dasatinib as a cancer drug. *Acta Biochimica et Biophysica Sinica*, *53*(7), 823–836. https://doi.org/10.1093/abbs/gmab061

Liu, S., Wang, X., Li, Y., Xu, L., Yu, X., Ge, L., Li, J., Zhu, Y., & He, S. (2014). Necroptosis mediates TNF-induced toxicity of hippocampal neurons. *BioMed Research International*, *2014*, 290182. https://doi.org/10.1155/2014/290182

Logan, S., Royce, G. H., Owen, D., Farley, J., Ranjo-Bishop, M., Sonntag, W. E., & Deepa, S. S. (2019). Accelerated decline in cognition in a mouse model of increased oxidative stress. *GeroScience*, *41*(5), 591–607. https://doi.org/10.1007/s11357-019-00105-y

Masternak, M. M., & Bartke, A. (2012). Growth hormone, inflammation and aging. *Pathobiology of Aging & Age Related Diseases*, *2*. https://doi.org/10.3402/pba.v2i0.17293

Miyata, T., Wu, X., Fan, X., Huang, E., Sanz-Garcia, C., Ross, C. K. C.-D., Roychowdhury, S., Bellar, A., McMullen, M. R., Dasarathy, J., Allende, D. S., Caballeria, J., Sancho-Bru, P., McClain, C. J., Mitchell, M., McCullough, A. J., Radaeva, S., Barton, B., Szabo, G., … Nagy, L. E. (2021). Differential role of MLKL in alcohol-associated and non–alcohol-associated fatty liver diseases in mice and humans. *JCI Insight*, *6*(4), e140180. https://doi.org/10.1172/jci.insight.140180

Mohammed, S., Nicklas, E. H., Thadathil, N., Selvarani, R., Royce, G. H., Kinter, M., Richardson, A., & Deepa, S. S. (2021). Role of necroptosis in chronic hepatic inflammation and fibrosis in a mouse model of increased oxidative stress. *Free Radical Biology & Medicine*, *164*, 315–328. https://doi.org/10.1016/j.freeradbiomed.2020.12.449

Mohammed, S., Thadathil, N., Selvarani, R., Nicklas, E. H., Wang, D., Miller, B. F., Richardson, A., & Deepa, S. S. (2021). Necroptosis contributes to chronic inflammation and fibrosis in aging liver. *Aging Cell*, *20*(12), e13512. https://doi.org/10.1111/acel.13512

Muller, F. L., Song, W., Liu, Y., Chaudhuri, A., Pieke-Dahl, S., Strong, R., Haung, T. T., Epstein, C. J., RobertsII, L. J., Csete, M., Faulkner, J. A., & Van Remmen, H. (2006). Absence of CuZn superoxide dismutase leads to elevated oxidative stress and acceleration of age-dependent skeletal muscle atrophy. *Free Radical Biology & Medicine*, *40*(11), 1993–2004. https://doi.org/10.1016/j.freeradbiomed.2006.01.036

Okado-Matsumoto, A., & Fridovich, I. (2001). Assay of superoxide dismutase: Cautions relevant to the use of cytochrome c, a sulfonated

tetrazolium, and cyanide. *Analytical Biochemistry*, *298*(2), 337–342. https://doi.org/10.1006/abio.2001.5385

Olivieri, F., Prattichizzo, F., Grillari, J., & Balistreri, C. R. (2018). Cellular senescence and inflammaging in age-related diseases. *Mediators of Inflammation*, *2018*, 9076485. https://doi.org/10.1155/2018/9076485

Olofsson, E. M., Marklund, S. L., & Behndig, A. (2007). Glucose-induced cataract in CuZn-SOD null lenses: An effect of nitric oxide?- *Free Radical Biology & Medicine*, *42*(7), 1098–1105. https://doi.org/10.1016/j.freeradbiomed.2007.01.012

Pang, Q., Jin, H., Qu, K., Man, Z., Wang, Y., Yang, S., Zhou, L., & Liu, H. (2017). The effects of nonsteroidal anti-inflammatory drugs in the incident and recurrent risk of hepatocellular carcinoma: A meta-analysis. *Oncotargets and Therapy*, *10*, 4645–4656. https://doi.org/10.2147/OTT.S143154

Park, E. J., Lee, J. H., Yu, G.-Y., He, G., Ali, S. R., Holzer, R. G., Osterreicher, C. H., Takahashi, H., & Karin, M. (2010). Dietary and genetic obesity promote liver inflammation and tumorigenesis by enhancing IL-6 and TNF expression. *Cell*, *140*(2), 197–208. https://doi.org/10.1016/j.cell.2009.12.052

Pasparakis, M., & Vandenabeele, P. (2015). Necroptosis and its role in inflammation. *Nature*, *517*(7534), 311–320. https://doi.org/10.1038/nature14191

Reaume, A., Elliott, J. L., Hoffman, E. K., Kowall, N. W., Ferrante, R. J., Siwek, D. R., Wilcox, H. M., Flood, D. G., Beal, M. F., Brown, R. H., Scott, R. W., & Snider, W. D. (1996). Motor neurons in Cu/Zn superoxide dismutase-deficient mice develop normally but exhibit enhanced cell death after axonal injury. *Nature Genetics*, *13*(1), 43–47. https://doi.org/10.1038/ng0596-43

Richardson, A., Galvan, V., Lin, A.-L., & Oddo, S. (2015). How longevity research can lead to therapies for Alzheimer's disease: The rapamycin story. *Experimental Gerontology*, *68*, 51–58. https://doi.org/10.1016/j.exger.2014.12.002

Sahasrabuddhe, V. V., Gunja, M. Z., Graubard, B. I., Trabert, B., Schwartz, L. M., Park, Y., Hollenbeck, A. R., Freedman, N. D., & McGlynn, K. A. (2012). Nonsteroidal anti-inflammatory drug use, chronic liver disease, and hepatocellular carcinoma. *Journal of the National Cancer Institute*, *104*(23), 1808–1814. https://doi.org/10.1093/jnci/djs452

Sakiyama, H., Fujiwara, N., Yoneoka, Y., Yoshihara, D., Eguchi, H., & Suzuki, K. (2016). Cu,Zn-SOD deficiency induces the accumulation of hepatic collagen. *Free Radical Research*, *50*(6), 666–677. https://doi.org/10.3109/10715762.2016.1164856

Smith, L. R., Hammers, D. W., Sweeney, H. L., & Barton, E. R. (2016). Increased collagen cross-linking is a signature of dystrophin-deficient muscle. *Muscle & Nerve*, *54*(1), 71–78. https://doi.org/10.1002/mus.24998

Snider, T. A., Richardson, A., Stoner, J. A., & Deepa, S. S. (2018). The Geropathology Grading Platform demonstrates that mice null for Cu/Zn-superoxide dismutase show accelerated biological aging. *GeroScience*, *40*(2), 97–103. https://doi.org/10.1007/s11357-018-0008-0

Spaulding, C. C., Walford, R. L., & Effros, R. B. (1997). Calorie restriction inhibits the age-related dysregulation of the cytokines TNF-alpha and IL-6 in C3B10RF1 mice. *Mechanisms of Ageing and Development*, *93*(1–3), 87–94. https://doi.org/10.1016/s0047-6374(96)01824-6

Takahashi, N., Duprez, L., Grootjans, S., Cauwels, A., Nerinckx, W., DuHadaway, J. B., Goossens, V., Roelandt, R., Van Hauwermeiren, F., Libert, C., Declercq, W., Yuan, J., & Vandenabeele, P. (2012). Necrostatin-1 analogues: Critical issues on the specificity, activity and in vivo use in experimental disease models. *Cell Death & Disease*, *3*, e437. https://doi.org/10.1038/cddis.2012.176

Tao, Y., Li, Y., Liu, X., Deng, Q., Yu, Y., & Yang, Z. (2018). Nonsteroidal anti-inflammatory drugs, especially aspirin, are linked to lower risk and better survival of hepatocellular carcinoma: A meta-analysis. *Cancer Management and Research*, *10*, 2695–2709. https://doi.org/10.2147/CMAR.S167560

Thadathil, N., Xiao, J., Hori, R., Alway, S. E., & Khan, M. M. (2021). Brain selective estrogen treatment protects dopaminergic neurons and preserves behavioral function in MPTP-induced mouse model of Parkinson's disease. *Journal of Neuroimmune Pharmacology*, *16*(3), 667–678. https://doi.org/10.1007/s11481-020-09972-1

Uchiyama, S., Shimizu, T., & Shirasawa, T. (2006). CuZn-SOD deficiency causes ApoB degradation and induces hepatic lipid accumulation by impaired lipoprotein secretion in mice. *The Journal of Biological Chemistry*, *281*(42), 31713–31719. https://doi.org/10.1074/jbc.M603422200

Vanlangenakker, N., Bertrand, M. J. M., Bogaert, P., Vandenabeele, P., & Vanden Berghe, T. (2011). TNF-induced necroptosis in L929 cells is tightly regulated by multiple TNFR1 complex I and II members. *Cell Death & Disease*, *2*, e230. https://doi.org/10.1038/cddis.2011.111

Villanueva, A., & Luedde, T. (2016). The transition from inflammation to cancer in the liver. *Clinical Liver Disease*, *8*(4), 89–93. https://doi.org/10.1002/cld.578

Wiley, C. D., & Campisi, J. (2021). The metabolic roots of senescence: Mechanisms and opportunities for intervention. *Nature Metabolism*, *3*(10), 1290–1301. https://doi.org/10.1038/s42255-021-00483-8

Woltman, A. M., Boonstra, A., Naito, M., & Leenen, P. J. M. (2014). Kupffer cells in health and disease. In Biswas, S. K. & Mantovani, A. (Eds.), *Macrophages: Biology and role in the pathology of diseases* (pp. 217–247). Springer. https://doi.org/10.1007/978-1-4939-1311-4_10

Xu, M., Pirtskhalava, T., Farr, J. N., Weigand, B. M., Palmer, A. K., Weivoda, M. M., Inman, C. L., Ogrodnik, M. B., Hachfeld, C. M., Fraser, D. G., Onken, J. L., Johnson, K. O., Verzosa, G. C., Langhi, L. G. P., Weigl, M., Giorgadze, N., LeBrasseur, N. K., Miller, J. D., Jurk, D., … Kirkland, J. L. (2018). Senolytics improve physical function and increase lifespan in old age. *Nature Medicine*, *24*(8), 1246–1256. https://doi.org/10.1038/s41591-018-0092-9

Yoon, S., Kovalenko, A., Bogdanov, K., & Wallach, D. (2017). MLKL, the protein that mediates necroptosis, also regulates endosomal trafficking and extracellular vesicle generation. *Immunity*, *47*(1), 51–65. e7. https://doi.org/10.1016/j.immuni.2017.06.001

Yu, L.-X., Ling, Y., & Wang, H.-Y. (2018). Role of nonresolving inflammation in hepatocellular carcinoma development and progression. *NPJ Precision Oncology*, *2*(1), 6. https://doi.org/10.1038/s41698-018-0048-z

Zhang, M., Tian, J., Wang, R., Song, M., Zhao, R., Chen, H., Liu, K., Shim, J. H., Zhu, F., Dong, Z., & Lee, M.-H. (2020). Dasatinib inhibits lung cancer cell growth and patient derived tumor growth in mice by targeting LIMK1. *Frontiers in Cell and Developmental Biology*, *8*, 556532. https://doi.org/10.3389/fcell.2020.556532

Zhang, Q., Raoof, M., Chen, Y., Sumi, Y., Sursal, T., Junger, W., Brohi, K., Itagaki, K., & Hauser, C. J. (2010). Circulating mitochondrial DAMPs cause inflammatory responses to injury. *Nature*, *464*(7285), 104–107. https://doi.org/10.1038/nature08780

Zhang, Y., Ikeno, Y., Bokov, A., Gelfond, J., Jaramillo, C., Zhang, H.-M., Liu, Y., Qi, W., Hubbard, G., Richardson, A., & Van Remmen, H. (2013). Dietary restriction attenuates the accelerated aging phenotype of Sod1−/− mice. *Free Radical Biology and Medicine*, *60*, 300–306. https://doi.org/10.1016/j.freeradbiomed.2013.02.026

Zhang, Y., Liu, Y., Walsh, M., Bokov, A., Ikeno, Y., Jang, Y. C., Perez, V. I., Van Remmen, H., & Richardson, A. (2016). Liver specific expression of Cu/ZnSOD extends the lifespan of Sod1 null mice. *Mechanisms of Ageing and Development*, *154*, 1–8. https://doi.org/10.1016/j.mad.2016.01.005

Zhang, Y., Unnikrishnan, A., Deepa, S. S., Liu, Y., Li, Y., Ikeno, Y., Sosnowska, D., Van Remmen, H., & Richardson, A. (2017). A new role for oxidative stress in aging: The accelerated aging phenotype

in Sod1−/− mice is correlated to increased cellular senescence. *Redox Biology*, *11*, 30–37. https://doi.org/10.1016/j.redox.2016.10.014

Zhao, Y.-J., Ju, Q., & Li, G.-C. (2013). Tumor markers for hepatocellular carcinoma. *Molecular and Clinical Oncology*, *1*(4), 593–598. https://doi.org/10.3892/mco.2013.119

Zhu, Y., Tchkonia, T., Pirtskhalava, T., Gower, A. C., Ding, H., Giorgadze, N., Palmer, A. K., Ikeno, Y., Hubbard, G. B., Lenburg, M., O'Hara, S P., LaRusso, N. F., Miller, J. D., Roos, C. M., Verzosa, G. C., LeBrasseur, N. K., Wren, J. D., Farr, J. N., Khosla, S., … Kirkland, J. L. (2015). The Achilles' heel of senescent cells: From transcriptome to senolytic drugs. *Aging Cell*, *14*(4), 644–658. https://doi.org/10.1111/acel.12344

SUPPORTING INFORMATION

Additional supporting information can be found online in the Supporting Information section at the end of this article.

How to cite this article: Thadathil, N., Selvarani, R., Mohammed, S., Nicklas, E. H., Tran, A. L., Kamal, M., Luo, W., Brown, J. L., Lawrence, M. M., Borowik, A. K., Miller, B. F., Van Remmen, H., Richardson, A., & Deepa, S. S. (2022). Senolytic treatment reduces cell senescence and necroptosis in Sod1 knockout mice that is associated with reduced inflammation and hepatocellular carcinoma. *Aging Cell*, *21*, e13676. https://doi.org/10.1111/acel.13676